Monthly Notices
of the
ROYAL ASTRONOMICAL SOCIETY

Mon. Not. R. Astron. Soc. **417,** 1387–1391 (2011) doi:10.1111/j.1365-2966.2011.19357.x

# *Suzaku* observation of the Galactic supernova remnant CTB 37A (G348.5+0.1)

A. Sezer,[1,2⋆] F. Gök,[3⋆] M. Hudaverdi[1⋆] and E. N. Ercan[2⋆]

[1]*TÜBİTAK Space Technologies Research Institute, ODTU Campus, Ankara, 06531, Turkey*
[2]*Boğaziçi University, Faculty of Art and Sciences, Department of Physics, Istanbul, 34342, Turkey*
[3]*Akdeniz University, Faculty of Sciences, Department of Physics, Antalya, 07058, Turkey*

Accepted 2011 June 29. Received 2011 June 24; in original form 2011 March 18

## ABSTRACT

In this paper, we present the results of the observations of CTB 37A obtained with the X-ray imaging spectrometer onboard the *Suzaku* satellite. The X-ray spectrum of CTB 37A is fitted well by two components: a single-temperature ionization equilibrium component (VMEKAL), with solar abundances, an electron temperature of $kT_e \sim 0.6$ keV and an absorbing column density of $N_H \sim 3 \times 10^{22}$ cm$^{-2}$, and a power-law component with a photon index of $\Gamma \sim 1.6$. The X-ray spectrum of CTB 37A is characterized by clearly detected K-shell emission lines of Mg, Si, S and Ar. The plasma with solar abundances supports the idea that the X-ray emission originates from the shocked interstellar material. The ambient gas density and the age of the remnant are estimated to be $\sim 1 f^{-1/2}$ cm$^{-3}$ and $\sim 3 \times 10^4 f^{1/2}$ yr, respectively. The centre-filling X-ray emission, surrounded by a shell-like radio structure, and other X-ray properties indicate that this remnant could be a new member of the class of mixed-morphology supernova remnants.

**Key words:** ISM: individual objects: CTB 37A – ISM: supernova remnants – X-rays: ISM.

## 1 INTRODUCTION

CTB 37A [also called G348.5+0.1, RA (2000) = $17^h\,14^m\,06^s$, Dec. (2000) = $-38°32'$] was discovered by Clark, Caswell & Green (1975) in the radio band. It has a shell-type morphology with an angular size of 15 arcmin. From Very Large Array observations at wavelengths of 6, 20, and 90 cm, Kassim, Baum & Weiler (1991) reported that this remnant is expanding in an inhomogeneous region, and is part of a complex composed of three supernova remnants (SNRs): CTB 37A, G348.7+0.3 (also called CTB 37B) and G348.5–0.0. From the *ASCA* Galactic plane survey data of G348.5+0.1, Yamauchi et al. (2008) found that the X-ray spectra of the SNR was heavily absorbed by interstellar matter with $N_H \sim 2 \times 10^{22}$ cm$^{-2}$ and the size of X-ray emission was comparable to its radio structure. Frail et al. (1996) detected OH masers with velocities at about 20 and 60 km s$^{-1}$, in the direction of CTB 37A at 1720 MHz. Reynoso & Mangum (2000) surveyed the environment of this remnant with associated OH 1720 MHz masers in the CO $J = 1$–0 transition with the 12-m telescope of the National Radio Astronomy Observatory (NRAO). They reported that a number of molecular clouds are interacting with the SNR shock fronts. Using *Chandra* and *XMM–Newton* data, Aharonian et al. (2008) have shown the presence of thermal X-rays from the north-east part, an extended non-thermal X-ray source, CXOU J171419.8–383023, in the north-west part and a gamma-ray source, HESS J1714–385, coincident with the remnant. They found a high absorbing column density of $N_H \sim 3 \times 10^{22}$ cm$^{-2}$. They claimed that the observed X-ray morphology was a result of the interaction with the inhomogeneous medium surrounding the remnant, and that this inhomogeneity was also responsible for the break-out radio morphology. Using observations with the *Fermi* Large Area Telescope (LAT), Castro & Slane (2010) have revealed gamma-ray emission from this SNR. The spectrum of the source coincident with CTB 37A was fitted by a power-law (PL) model with an exponential cut-off at energy $E_{cut} = 4.2$ GeV. Considering the lack of evidence for contribution by a pulsar and the presence of maser emission for the remnant, they proposed that gamma-rays result from interactions between the SNR and molecular clouds.

The distance to CTB 37A has been estimated from 21-cm absorption measurements to be between 6.7 and 13.7 kpc by Caswell et al. (1975). From velocity measurements of molecular clouds associated with the remnant, Reynoso & Mangum (2000) adopted a distance of 11.3 kpc. So, we use $d = 11.3$ kpc for our calculations throughout this paper.

CTB 37A is an interesting and important SNR because of its location, which contains OH maser sources (Frail et al. 1996), 1FGL J1714.5–3830 (Castro & Slane 2010), the X-ray source CXOU J171419.8-383023 and HESS J1714–385 (Aharonian et al. 2008), as well as two additional SNRs, G348.5–0.0 and G348.7+0.3. In addition, its morphology implies a similarity to the recently

⋆E-mail: aytap.sezer@uzay.tubitak.gov.tr (AS); gok@akdeniz.edu.tr (FG); murat.hudaverdi@uzay.tubitak.gov.tr (MH); ercan@boun.edu.tr (ENE)

© 2011 The Authors
Monthly Notices of the Royal Astronomical Society © 2011 RAS

Downloaded from https://academic.oup.com/mnras/article/417/2/1387/984597 by Yildiz Teknik University Library (YTU) user on 25 February 2022

proposed group of mixed-morphology (MM) SNRs, increasing its importance. High-quality imaging and spectra obtained from the data provided by the X-ray observatory *Suzaku* are used to produce the results in this work.

The organization of this paper is as follows. We describe the *Suzaku* X-ray observations of CTB 37A, including details of data reduction in Section 2. The image and spectral analyses are given in Sections 3 and 4, respectively. Finally, in Section 5, we consider the morphology of CTB 37A and we investigate the radial variations of the electron temperature. Then, we discuss the implications of the MM class and the nature of the thermal and non-thermal components of CTB 37A.

## 2 OBSERVATION AND DATA REDUCTION

*Suzaku* (Mitsuda et al. 2007) is the fifth Japanese X-ray astronomy satellite, which was launched on 2005 July 10. *Suzaku* observed CTB 37A on 2010 February 20. The observation ID and exposure time are 504097010 and 53.8 ks, respectively. The X-ray imaging spectrometer (XIS; Koyama et al. 2007) consists of four sets of X-ray CCD camera system (XIS0, XIS1, XIS2 and XIS3). XIS0, XIS2 and XIS3 have front-illuminated (FI) sensors, and provide coverage over the energy range 0.4–12 keV. XIS1 has a back-illuminated (BI) sensor, which provides greater sensitivity at lower energies (0.2–12 keV). The XIS has a field of view (FOV) of 17.8 × 17.8 arcmin$^2$ (1024 × 1024 pixels). Each XIS CCD has an $^{55}$Fe calibration source, which can be used to calibrate the gain and to test the spectral resolution of data taken using this instrument. The XIS2 sensor was available only until 2006; therefore, we use the data of XIS0, XIS1, XIS3.

Reduction and analysis of the data were performed following the standard procedure, using the HEADAS software package, version 6.5. Spectral fitting was performed with XSPEC, version 11.3.2 (Arnaud 1996). The XIS was operated in the normal full-frame clocking mode, with the standard 3 × 3 and 5 × 5 editing modes. We generated XIS response matrices using the XISRMFGEN software, which takes into account the time-variation of the energy response. As for generating ancillary response files (ARFs), we used XISSIMARFGEN (Ishisaki et al. 2007). The latest versions of the relevant *Suzaku* CALDB files were also used.

## 3 IMAGE ANALYSIS

Fig. 1 shows an XIS1 image in the 0.3–10 keV energy band. We have extracted the spectrum from the brightest region, represented with the outermost solid circle centred at RA (2000) = $17^h\ 14^m\ 30^s$, Dec. (2000) = $-38°32'07''$ with a radius of 5.5 arcmin. To derive the radial variation of the electron temperature $kT_e$, we take four apertures with sizes of 0–1.5, 1.5–2.5, 2.5–3.5 and 3.5–4.5 arcmin. The extended non-thermal X-ray source (CXOU J171419.8–383023), shown by the solid red circle, is excluded from the spectral analysis. The dashed black circle centred at [RA (2000) = $17^h\ 14^m\ 19^s$, Dec. (2000) = $-38°24'36''$ with radius 1.7 arcmin] represents the background region. In the lower-left corner, shown by a dashed red circle, the FOV that contains the calibration source emission is extracted.

Fig. 2 shows the XIS0 image in the 0.3–10 keV energy band, which is overlaid with the radio image obtained at 843 MHz by Whiteoak & Green (1996) for comparison. Blue crosses indicate the direction of the detected OH (1720 MHz) maser emission at velocities $\sim -65$ km s$^{-1}$ associated with CTB 37A. White crosses show the positions of maser emission at velocities $\sim -22$ km s$^{-1}$

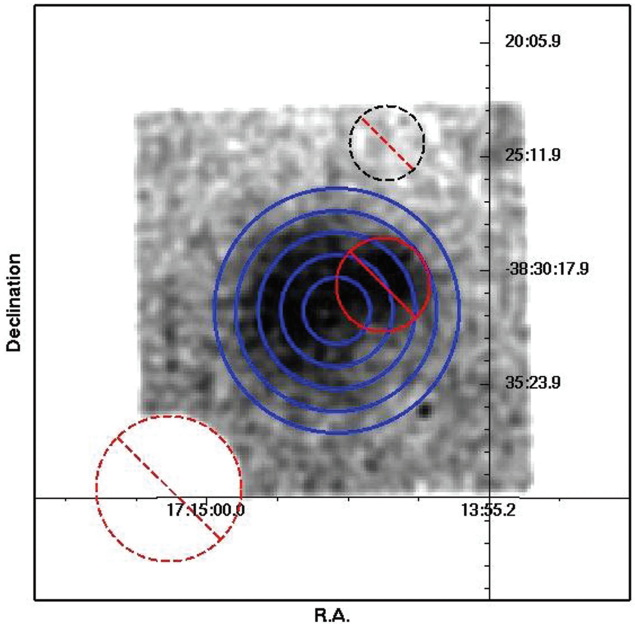



**Figure 1.** *Suzaku* XIS1 image of CTB 37A in the 0.3–10 keV energy band. The spectral integration regions for the source (annular apertures) and the background are indicated by the solid blue and dashed black circles, respectively. The solid red circle represents the X-ray source (CXOU J171419.8–383023). The corner of the CCD chip illuminated by the $^{55}$Fe calibration source is excluded from the image as shown by the dashed red circle. The coordinates (RA and Dec.) refer to epoch J2000.

(Frail et al. 1996). The diamond indicates the position of CXOU J171419.8–383023, and the circle represents the location of HESS J1714–385 (Aharonian et al. 2008).

## 4 SPECTRAL ANALYSIS

The XIS spectra were extracted, using XSELECT version 2.4a, from XIS0–XIS3 with a circular extraction region of radius 5.5 arcmin. These are grouped with a minimum of 50 counts bin$^{-1}$. We fit the spectra with a collisional ionization equilibrium (CIE) model with variable abundances (XSPEC model 'VMEKAL'; Mewe, Gronenschild & van den Oord 1985; Mewe, Lemen & van den Oord 1986; Liedahl, Osterheld & Goldstein 1995) modified by interstellar absorption (wabs in XSPEC; Morrison & McCammon 1983). The parameters of the absorbing column density ($N_H$) and electron temperature ($kT_e$) are set free, while all elements are fixed at solar abundances (Anders & Grevesse 1989). The best-fitting reduced $\chi^2$/d.o.f. for this model is 2222.5/832 = 2.67. To find out if there was any contribution from non-thermal emission, we added a PL component (VMEKAL+PL), which yields a better reduced $\chi^2$ of 935.5/830 = 1.13. Then, the Mg, Si, S and Ar lines in the spectrum were set free, while the rest were fixed at their solar values. We found insignificant improvement in the $\chi^2$ value (891.6/826 = 1.08). Therefore, we decided to fix the abundances of Mg, Si, S and Ar at their solar values. In Table 1, we present the best-fitting parameters and the statistics obtained with an absorbed VMEKAL+PL, with corresponding errors at the 90 per cent confidence level ($2.7\sigma$). Fig. 3 shows the spectra of XIS0, XIS1 and XIS3 simultaneously, in the energy range of 0.3–10 keV, which is taken from the region shown by the solid (outermost) blue circle presented in Fig. 1. We performed annular spectral analysis for the four regions shown by the circles in Fig. 1 in order to derive the radial temperature

Downloaded from https://academic.oup.com/mnras/article/417/2/1387/984597 by Yildiz Teknik University Library (YTU) user on 25 February 2022

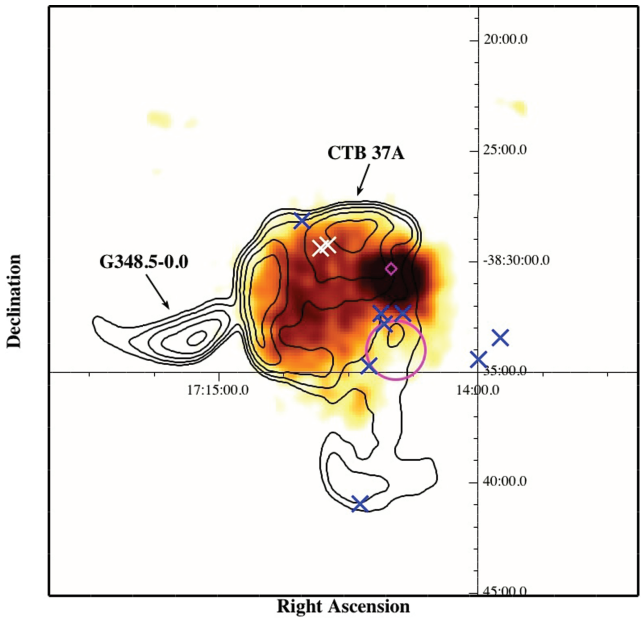



**Figure 2.** CTB 37A is displayed in the 0.3–10 keV energy band, with X-ray data obtained from the *Suzaku* XIS0 detector. The image is overlaid by 843-MHz radio isocontours logarithmically scaled (0.23, 0.36, 0.57, 0.90, 1.42, 2.23 and 3.51 mJy beam$^{-1}$). Radio emission clearly shows two radio SNRs, CTB 37A and G348.5–0.0. The X-ray data are smoothed with a three-pixel Gaussian in order to highlight the structure. The colour coding shows the brightness levels from 1.3 counts pix$^{-1}$ to 13.36 counts pix$^{-1}$ in logarithmic scale from yellow to black. The masers from the field are indicated with blue and white crosses at velocities $\sim-65$ and $\sim-22$ km s$^{-1}$, respectively. The diamond shows the extended non-thermal X-ray source CXOU J171419.8–383023. The location of HESS J1714–385 is represented by the circle, in which the positional error is specified with the radius of 1.2 arcmin. The coordinates (RA and Dec.) refer to epoch J2000.

variations of CTB 37A. The annular regions are spaced by 1 arcmin from the innermost circle with radius $r = 1.5$ arcmin. The VMEKAL+PL spectral model was also fitted to each annulus. While fitting these, we kept the absorbing column density $N_{\rm H}$ at its best-fitting value for the entire remnant. Fig. 4 shows the electron temperature variations with respect to the radius.

## 5 DISCUSSION AND CONCLUSIONS

In this paper, we have provided a description of the X-ray emission of CTB 37A based on *Suzaku* archival data. We obtained a clear image and high-quality spectra of diffuse X-ray emission. We have examined the thermal and non-thermal emissions coming from the remnant. The X-ray spectrum of CTB 37A is characterized by thermal emission, dominated by K-shell emission lines of Mg, Si, S and Ar, which are clearly detected.

As seen from Fig. 2, the radio emission of CTB 37A comprises a partial shell towards the north and east, and an extended outbreak to the south. The X-ray emission has a deformation along the south-west limb, where the morphology appears indented. The reason for such a deformation could be because of the inhomogeneous medium along this specific region. This may well be supported by the fact that the remnant is close to the Galactic plane and several OH masers at 1720 MHz (shown by crosses) are detected towards CTB 37A (Frail et al. 1996). Also, the gamma-ray emission could be relevant, as it is thought to be associated with the interaction between CTB 37A and the dense surrounding material that has been detected with the *Fermi* LAT (Castro & Slane 2010).

**Table 1.** Best-fitting parameters and $\chi^2$ values of the spectral fitting in the full energy band (0.3–10 keV) with an absorbed VMEKAL+PL model with corresponding errors at the 90 per cent confidence level ($2.7\sigma$).

| Component | Parameters | VMEKAL+PL |
|---|---|---|
| Wabs | $N_{\rm H}$ ($\times10^{22}$ cm$^{-2}$) | $2.9 \pm 0.1$ |
| VMEKAL | $kT_{\rm e}$ (keV) | $0.63 \pm 0.02$ |
| Abundance[a] | Mg | (1) |
| | Si | (1) |
| | S | (1) |
| | Ar | (1) |
| | VEM[b] | $72.3 \pm 2.1$ |
| | Flux[c] | $1.36 \pm 0.03$ |
| PL | Photon index | $1.6 \pm 0.1$ |
| | Norm ($\times10^{-2}$ photons cm$^{-2}$ s$^{-1}$) | $1.9 \pm 0.2$ |
| | Flux[d] | $1.5 \pm 0.1$ |
| | $\chi^2$/d.o.f. | $935.6/830 = 1.13$ |

[a](1) indicates that the elemental abundance is fixed at solar (Anders & Grevesse 1989).
[b]Volume emission measure VEM $= \int n_{\rm e} n_{\rm H}\, {\rm d}V$ in units of $10^{58}$ cm$^{-3}$, where $n_{\rm e}$ and $n_{\rm H}$ are the number densities of electrons and protons, respectively, and $V$ is the X-ray emitting volume.
[c]Unabsorbed flux in the 0.3–10 keV energy band in units of $10^{-9}$ erg s$^{-1}$ cm$^{-2}$.
[d]Total unabsorbed flux of the sum of the VMEKAL and PL components in the 0.3–10 keV energy band in units of $10^{-9}$ erg s$^{-1}$ cm$^{-2}$.

### 5.1 Implications for mixed morphology

SNRs were originally divided into shell-like, Crab-like (plerionic) and composite (shell-like containing plerions) remnants (Seward 1985), according to their X-ray morphology. Recently, an additional MM class (also called thermal composite) has appeared. These SNRs are centre-filled in X-rays and are shell-like at radio wavelengths (Seward 1990; Jones et al. 1998; Rho & Petre 1998). As seen from Fig. 2, CTB 37A has a shell-like morphology in the radio band while being centrally filled in the X-ray band; thus, our first impression is that CTB 37A seems to be a MM SNR. Examples of well-known MM SNRs include W28 (Rho & Borkowski 2002), G290.1–0.8 (Slane et al. 2002) and IC 443 (Kawasaki et al. 2002). Lazendic & Slane (2006) have reported important results about this class by compiling a list of 26 MM SNRs.

The X-ray characteristics of MM remnants have been defined by Rho & Petre (1998) as follows. (i) The radial temperature distribution is relatively flat. (ii) The X-ray emission arises primarily from shocked interstellar material, and not from ejecta. (iii) The remnants are typically located close to molecular clouds or very dense regions. (iv) The dominant X-ray emission is thermal in nature. Subsequent studies have indicated that MM SNRs have a complex plasma structure with multiple components (e.g. Rho & Borkowski 2002) and enhanced abundances (e.g. Yamauchi et al. 1999; Slane et al. 2002). They have evolved over $\sim10^4$ yr, which means that the plasma is in CIE or an overionization condition (Kawasaki et al. 2005). As can be seen from Fig. 4, the annular analysis of CTB 37A could be indicating a very small-scale radial variation in its temperature between the selected regions. The best-fitting metal abundances are found to be solar in general, confirming the absence of ejecta contamination in selected regions. This could support the idea that the X-ray emission originates from the shocked interstellar material. The plasma of CTB 37A is in a collisional ionization



Downloaded from https://academic.oup.com/mnras/article/417/2/1387/984597 by Yildiz Teknik University Library (YTU) user on 25 February 2022

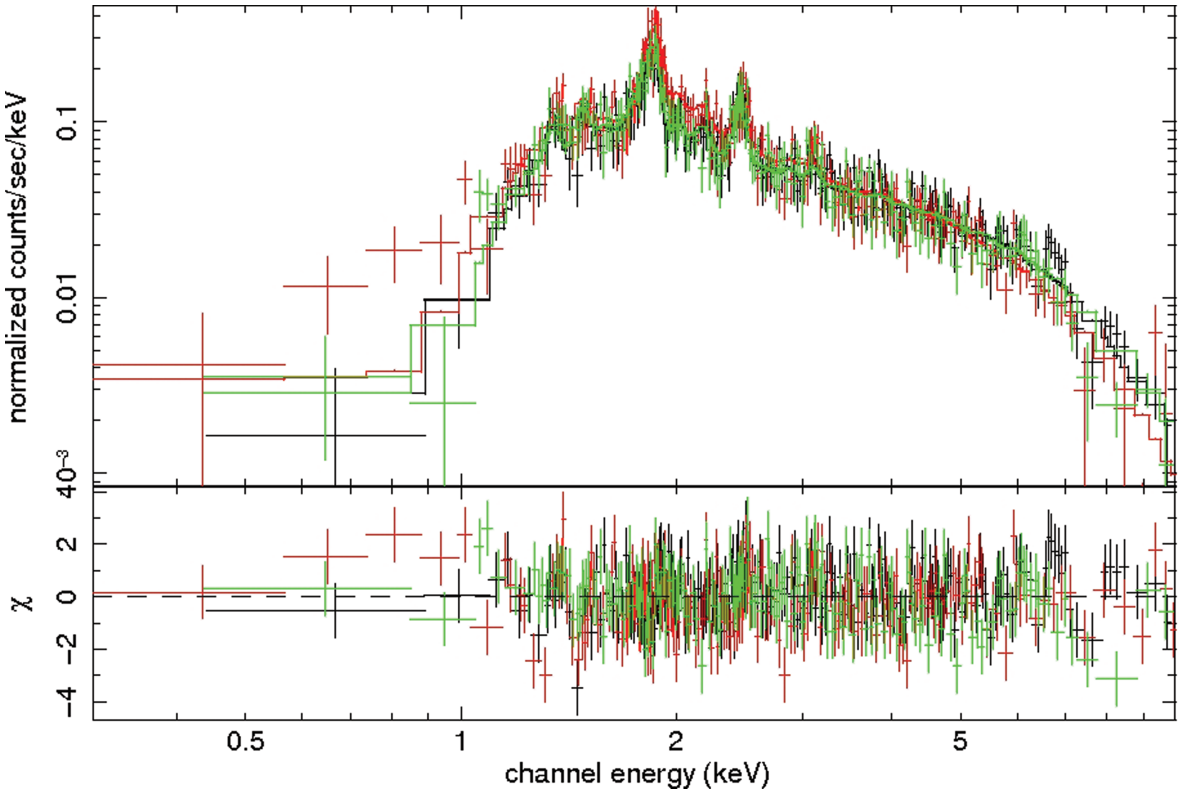



**Figure 3.** Background-subtracted XIS spectra of CTB 37A in the 0.3–10 keV energy band fitted with an absorbed VMEKAL and PL model. XIS1, XIS0 and XIS3 are shown in red, black and green, respectively. The bottom panel shows the residuals from the best-fitting model.

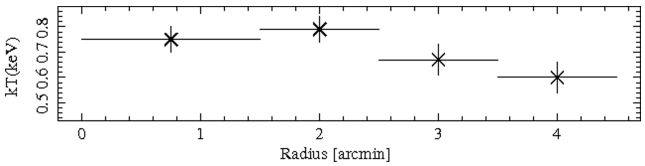



**Figure 4.** The radial variation of the electron temperature of CTB 37A.

equilibrium condition. It is located in a region with density variation, possibly associated with molecular clouds. The plasma has thermal and non-thermal emission, but the emission is dominated by the thermal component (∼90 per cent of the total X-ray flux). These X-ray properties of CTB 37A exemplify the typical characteristics of MM SNRs, as defined by Rho & Petre (1998).

There are a few models that can produce centrally enhanced X-ray emission. One is the evaporation of clouds left relatively unspoilt after the passage of the SNR blast wave (e.g. White & Long 1991). Another is 'fossil' thermal radiation, which is detectable as thermal X-rays from the hotter interior as the shell of an expanding SNR cools below $\sim 10^6$ K and becomes invisible as a result of interstellar absorption (e.g. Seward 1985). As the SNR evolves, the temperature and density of the hot interior plasma gradually become uniform through thermal conduction (e.g. Cox et al. 1999) or evolution in a medium with a density gradient viewed along the line of sight (Petruk 2001). The evaporation model requires dense clouds. The thermal conduction model requires a relatively high-density ambient medium. CTB 37A is located in a region of greatly varying density, with OH maser sources indicating interaction with molecular clouds. Thus, the centre-filled X-ray morphology of CTB 37A is consistent with the model of evaporating clouds. The radial temperature variation in the plasma of CTB 37A ($kT_e \sim$ 0.6–0.8 keV) is consistent with other MM SNRs, such as W44 (Rho et al. 1994; Shelton, Kuntz & Petre 2004), 3C391 (Rho & Petre 1996; Chen et al. 2004) and HB21 (Pannuti et al. 2010). The very small temperature variation in the plasma of CTB 37A (as shown Fig. 4) can be explained by both evaporation and thermal conduction models. Future deep X-ray observations and detailed spectral analysis of this remnant will give more detailed information for comparison with theoretical models that produce MM SNRs.

### 5.2 Thermal component

The X-ray emission of CTB 37A is dominated by thermal emission that can best be described by an absorbed CIE plasma model (VMEKAL) with an absorbing column density of $N_H \sim 3 \times 10^{22}$ cm$^{-2}$, an electron temperature of $kT_e \sim 0.6$ keV and solar abundances of Mg, Si, S and Ar, which indicate a shocked interstellar/circumstellar medium origin.

For full ionization equilibrium, the ionization time-scale, $\tau = n_e\, t$, should be $\geq 10^{12}$ cm$^{-3}$ s, where $t$ is the plasma age or the time since the gas was shock-heated (Masai 1984). To determine the age of the remnant, $n_e$ should be estimated from the emission measure, $n_e\, n_H\, V$, which is related to the normalization of the VMEKAL model according to the following equation, norm $= n_e\, n_H\, V/(4\pi\, d^2 \times 10^{14})$. Here, $V$ is the X-ray emitting volume, $n_H$ is the volume density of hydrogen and $d$ is the distance. For simplicity, we have assumed that the emitting region is a sphere of radius 5.5 arcmin. Considering the possibility that less than the entire volume is filled, we write the volume $V = V_s\, f$, where $V_s$ is the full spherical volume and $f$ is the filling factor. We then carry the $f$ factor through our calculations to show the explicit dependence of each derived quantity on this factor. Knowing that the SNR is at a distance of

Downloaded from https://academic.oup.com/mnras/article/417/2/1387/984597 by Yildiz Teknik University Library (YTU) user on 25 February 2022

11.3 kpc and $n_e = 1.2n_H$, we estimated the emission volume to be $V \sim 6.7 \times 10^{59} f\ cm^3$. Consequently, we find an ambient gas density of $\sim 1 f^{-1/2}\ cm^{-3}$ and an age of $\sim 3 \times 10^4 f^{1/2}$ yr (assuming $n_e\ t \sim 1 \times 10^{12}\ cm^{-3}$ s). This implies that CTB 37A is a middle-aged SNR. Finally, we calculated the total mass of the X-ray emitting plasma, $M_x$, by $M_x = m_H\ n_e\ V \sim 530\ f^{1/2}\ M_\odot$, where $m_H$ is the mass of a hydrogen atom and $\mu = 0.604$ is the mean atomic weight.

### 5.3 Power-law component

The *Suzaku* X-ray spectral data of CTB 37A are well fitted with a thermal component and an additional hard component. There could be a few reasons for the hard X-ray emission: (i) an association with a classical young pulsar; (ii) a contribution from an extended non-thermal X-ray source (CXOU J171419.8–383023); (iii) overionization of the plasma, which produces excess hard emission, as is the case for IC443 (Yamaguchi et al. 2009). The hard component is well fitted by a PL model with a photon index value of ∼1.6. This value is consistent with that of a classical young pulsar value ranging between 1.1 and 1.7 (Chakrabarty et al. 2001). However, there is no pulsar reported that is associated with this remnant. In the north-west region of CTB 37A, an extended non-thermal X-ray source (CXOU J171419.8–383023) is reported [RA (2000) = $17^h\ 14^m\ 20^s$, Dec. (2000) = $-38°30'20''$] by Aharonian et al. (2008), who found non-thermal emission from the source with a spectral index of ∼1.32, which is lower (harder) than our best-fitting value of ∼1.6. Although we excluded CXOU J171419.8–383023 (with a radius of 2.1 arcmin) from our spectra during our spectral analysis, our fits require a non-thermal component. To investigate this, we also performed spectral analysis for individual regions by selecting small rectangular regions that are further away from the known extended non-thermal source. The non-thermal flux is found to be stronger for the selected small regions nearby the source compared to those further away. We have obtained an unabsorbed flux value of $F_x \sim 1.4 \times 10^{-9}$ erg $s^{-1}$ $cm^{-2}$ for the non-thermal extended source in the 0.3–10 keV energy range. When we compare this with the unabsorbed flux value ($F_x \sim 0.14 \times 10^{-9}$ erg $s^{-1}$ $cm^{-2}$) of the best-fitting PL component, we find a factor of 10 difference between them. This difference indicates that the extended source is most likely the origin of the PL component and the emission is scattered from the source into the field of the rest of the remnant by a broad point spread function of the *Suzaku* mirrors.

The spectral studies of CTB 37A indicate that the plasma is best described by a thermal component in CIE condition with solar elemental abundances and a non-thermal component with a photon index of ∼1.6. The thermal emission possibly originates from the shocked interstellar material with an ambient gas density of $\sim 1 f^{-1/2}$ $cm^{-3}$. The best spectral fits require an ionization time-scale of $\tau \geq 10^{12}\ cm^{-3}$ s, implying an age of $\sim 3 \times 10^4 f^{1/2}$ yr. The origin of the power-law component is more likely the effect of the contribution from the extended source (CXOU J171419.8–383023) located in the north-west part of the remnant. CTB 37A is most likely a new member of the MM SNRs.

## ACKNOWLEDGMENTS

We thank Dr Patrick Slane for his valuable comments and suggestions, which have helped to improve the overall quality of the manuscript. AS is supported by a TÜBİTAK post-doctoral fellowship. This work is supported by the Akdeniz University Scientific Research Project Management and by TÜBİTAK under project codes 108T226 and 109T092. The authors also acknowledge the support by the Boğaziçi University Research Foundation under the 2010 Scientific Research Project Support (BAP) project no. 5052.

## REFERENCES

Aharonian F. et al., 2008, A&A, 490, 685
Anders E., Grevesse N., 1989, Geochim. Cosmochim. Acta, 53, 197
Arnaud K. A., 1996, in Jacoby G., Barnes J., eds, ASP Conf. Ser. Vol. 101, Astronomical Data Analysis Software and Systems V. Astron. Soc. Pac., San Francisco, p. 17
Castro D., Slane P., 2010, ApJ, 717, 372
Caswell J. L., Murray J. D., Roger R. S., Cole D. J., Cooke D. J., 1975, A&A, 45, 239
Chakrabarty D., Pivovaroff M. J., Hernquist L. E., Heyl J. S., Narayan R., 2001, ApJ, 548, 800
Chen Y., Su Y., Slane P. O., Wang Q. D., 2004, ApJ, 616, 885
Clark D. H., Caswell J. L., Green A. J., 1975, Australian J. Phys., Astrophys. Suppl., 37, 1
Cox D. P., Shelton R. L., Maciejewski W., Smith R. K., Plewa T., Pawl A., Różyczka M., 1999, ApJ, 524, 179
Frail D. A., Goss W. M., Reynoso E. M., Giacani E. B., Green A. J., Otrupcek R., 1996, AJ, 111, 1651
Ishisaki Y. et al., 2007, PASJ, 59, 113
Jones T. W. et al., 1998, PASP, 110, 125
Kassim N. E., Baum S. A., Weiler K. W., 1991, ApJ, 374, 212
Kawasaki M. T., Ozaki M., Nagase F., Masai K., Ishida M., Petre R., 2002, ApJ, 572, 897
Kawasaki M., Ozaki M., Nagase F., Inoue H., Petre R., 2005, ApJ, 631, 935
Koyama K. et al., 2007, PASJ, 59, 23
Lazendic J. S., Slane P. O., 2006, ApJ, 647, 350
Liedahl D. A., Osterheld A. L., Goldstein W. H., 1995, ApJ, 438, L115
Masai K., 1984, Ap&SS, 98, 367
Mewe R., Gronenschild E. H. B. M., van den Oord G. H. J., 1985, A&AS, 62, 197
Mewe R., Lemen J. R., van den Oord G. H. J., 1986, A&AS, 65, 511
Mitsuda K. et al., 2007, PASJ, 59, 1
Morrison R., McCammon D., 1983, ApJ, 270, 119
Pannuti T. G., Rho J., Borkowski K. J., Cameron P. B., 2010, AJ, 140, 1787
Petruk O., 2001, A&A, 371, 267
Reynoso E. M., Mangum J. G., 2000, ApJ, 545, 874
Rho J., Borkowski K. J., 2002, ApJ, 575, 201
Rho J., Petre R., 1996, ApJ, 467, 698
Rho J., Petre R., 1998, ApJ, 503, L167
Rho J., Petre R., Schlegel E. M., Hester J. J., 1994, ApJ, 430, 757
Seward F. D., 1985, Comments Astrophys. XI, 1, 15
Seward F. D., 1990, ApJS, 73, 781
Shelton R. L., Kuntz K. D., Petre R., 2004, ApJ, 611, 906
Slane P., Smith R. K., Hughes J. P., Petre R., 2002, ApJ, 564, 284
White R. L., Long K. S., 1991, ApJ, 373, 543
Whiteoak J. B. Z., Green A. J., 1996, A&AS, 118, 329
Yamaguchi H., Ozawa M., Koyama K., Masai K., Hiraga J. S., Ozaki M., Yonetoku D., 2009, ApJ, 705, L6
Yamauchi S., Koyama K., Tomida H., Yokogawa J., Tamura K., 1999, PASJ, 51, 13
Yamauchi S., Ueno M., Koyama K., Bamba A., 2008, PASJ, 60, 1143

This paper has been typeset from a TEX/LATEX file prepared by the author.

Downloaded from https://academic.oup.com/mnras/article/417/2/1387/984597 by Yildiz Teknik University Library (YTU) user on 25 February 2022